Morphology of nascent melt polymerized poly(2,6-oxynaphthoate/*m*-oxybenzoate) copolymer*

F. Rybnikar, B.-L. Yuan and P. H. Geil†
Department of Materials Science and Engineering and Materials Research Laboratory, University of Illinois at Urbana-Champaign, 1304 West Green Street, Urbana, IL 61801, USA
(Received 10 June 1993; revised 18 September 1993)

The 1/1 copolymer of *meta*-acetoxybenzoic acid and 2,6-acetoxynaphthoic acid (ANA), prepared by constrained thin film polymerization, crystallizes from the liquid crystal state during polymerization as single disclination domains and lamellar single crystals in the thinnest regions. Lamellae are also seen in the thicker regions. A sublimation–recrystallization–melting–polymerization–crystallization process occurs isothermally, at temperatures below the melting point of the ANA. Infra-red spectra confirm the polymerization and indicate the presence of both monomers. Electron diffraction from the single crystals indicates a phase I structure, similar to that in poly(*p*-oxybenzoate), with a doubling of the *b* axis dimension in some crystals. Electron diffraction from sheared samples, after annealing, suggests formation of poly(oxynaphthoate) blocks; the as-sheared samples have only a single *c* axis reflection (2.1 Å).

(Keywords: morphology; copolymer; melt polymerization)

INTRODUCTION

We have recently described techniques for growing lamellar single crystals of poly(*p*-oxybenzoate) (P*p*OBA)[1] and poly(2,6-oxynaphthoate) (PONA)[2,3] homopolymers in constrained thin films. This technique has been extended to homo- and copolymers, for all pairs, of *p*-, *m* and *o*OBA, ONA and 4-4′-oxybibenzoate (OBBA), using, in all cases, the acetoxy-acid monomer[4–7]. Although there are several papers describing the structure of P(*p*OBA/*m*OBA) copolymer and its change during heating, using electron diffraction (e.d.) from sheared samples[8–10], we know of no papers describing either the morphology of those samples as polymerized or the structure and morphology of P(ONA/*m*OBA) copolymers. In this paper we describe our results for P(ONA/*m*OBA) copolymers polymerized in constrained films as well as by bulk solution polymerization. Papers describing detailed results for the other copolymers are in preparation.

EXPERIMENTAL

meta-Hydroxybenzoic acid was purchased from Aldrich, 2,6-hydroxynaphthoic acid was supplied by Hoechst-Celanese. Both monomers were acetylated as described in ref. 2; the melting points of *meta*-acetoxybenzoic acid (*m*ABA) and 2,6-acetoxynaphthoic acid (ANA) were 135 and 226°C, respectively, as measured in a Perkin–Elmer DSC-4 at 20°C min^{-1} heating rate.

The copolymer was prepared either in 1-chloronaphthalene solution, ~15% w/v concentration, at 235°C or between glass on a hot plate at 180 or 200°C with, nominally, 3/1, 1/1 and 1/3 mole ratios. For the constrained thin film preparations the monomers were first codissolved in acetone, cast on glass cover slips from dilute solution and, following drying, sandwiched with another (clean) cover slip and wrapped in aluminium foil. Polymerization was done on a thermostatted hot plate for various times. Temperature was controlled to ±1°C. The slides were then separated, washed in acetone to remove any residual low molecular weight polymer and monomer, shadowed with Pt-C if desired, coated with carbon and either stripped, as a replica, with polyacrylic acid or floated on HF to permit e.d. Gold was used to calibrate the e.d. patterns. The bulk solution prepared material was also washed with acetone before further examination. Similar thin film samples, without the aluminium foil, were used for observation on the hot stage of an optical microscope. For i.r. and thermal analysis, thicker films were cast on glass slides and treated as above. All of the cast films varied in thickness and possibly in composition within a given film, the outer boundary being thicker than the centre.

A Jeol-100C transmission electron microscope was used for TEM and e.d. A 3 μm diameter aperture was used for the selected area patterns. Optical microscopy was done using a Reichert Zetopan microscope with a Kofler hot stage. Thermal analysis was done with a Perkin–Elmer DSC-4, on solution prepared material and on sample scrapped from several slides. I.r. scans were run on similar samples, in KBr pellets, on a Perkin–Elmer 1600 FTIR. The samples were scrapped from the thicker regions of the films from several slides.

* Presented at 'International Polymer Physics Symposium Honouring Professor John D. Hoffman's 70th Birthday', 15–16 May 1993, Washington, DC, USA
† To whom correspondence should be addressed

0032-3861/94/09/1831–15

RESULTS

Optical microscopy

The constrained film polymers described here were all polymerized below the melting point of the ANA, as measured by d.s.c. However, as shown by the optical microscopy described below and by d.s.c. measurements of bulk samples of ANA that had been held at similar temperatures for an extended period[3], both sublimation and a chemical reaction occur, resulting in material that is molten at the polymerization temperature. Thus, even though the ANA and *m*-ABA may crystallize independently during casting, both are molten and, apparently, mixed. We also note here, as in ref. 1 (see also ref. 11), that the reaction and melting, at a given temperature, occur much more rapidly between the slides than in a bulk sample (5 g) in a test tube. The chemical nature of the material formed in this reaction, from which polymerization actually occurs, is still under investigation.

Figure 1 shows representative optical micrographs of the 1/1 sample taken as a thin sample which was heated over a period of about 30 min to 180°C and then held there for 17 h. The initial sample consisted of small birefringent crystals near the centre of the spot of cast film (the macroscopic orientation is presumably due to the rubbing direction during cleaning of the glass) (*Figure 1b*) and a mixture of small crystals and structureless thick regions near the outer edge (*Figure 1a*). Melting began at about 110°C, well below the melting temperature, T_m, of even *m*ABA (135°C), the spot becoming transparent to the edge even though birefringence remained (*Figure 1d*). The sample, however, had liquid-like domains in transmitted light (*Figure 1c*). The transmitted light photos were 'shadowed' by partially inserting the analyser slide opening. Thin, large, lath-like crystals of low birefringence developed on the upper cover glass at about 110°C and then melted at slightly higher temperatures (124°C). These crystals grew in and past (by sublimation) the droplets of liquid on the upper glass.

At about 150°C a second type of lath-like crystal started to grow, again by a sublimation/recrystallization process on both the top and bottom glass (and, in some cases, on the glass bridge cover) of the cover slip sandwich (*Figures 1d* and *e*). The liquid-like domains also increased in size (*Figure 1f*). Regions of melt in contact with both surfaces are outlined by the black lines. It was noted that in ANA and *p*ABA heated at similar rates, similar lath-like crystals also formed, but at temperatures near 200 and 180°C, respectively. These crystals continued to grow as the temperature was raised to 183°C, the small, solvent-cast, original crystals disappearing (*Figure 1g*). They also grew if the sample temperature was held constant. In the regions containing the rows of small crystals (as in *Figures 1b* and *e*), individual laths started to grow at various locations, also at about 150°C, the crystals around them melting.

This sample was then held at about 180°C. *Figures 1h* and *i*, taken 15 min after *Figure 1g*, show the start of polymerization (small dots, each with a cross at the centre between crossed polars) developing. Simultaneously the large lath-like crystals slowly melted. In the central region of the film, the dots developed throughout (*Figure 1j*). In *Figure 1i*, each of the dots is seen to be a small mound.

Approximately 3 h later, when next observed, there was a complete change in appearance. The area corresponding to *Figures 1b* and *j* consisted of a number of single disclination domains (*Figure 1k*). Focus was difficult because the polymer formed on the two surfaces. The long birefringent domain at upper left corresponds to the location of a single lath-like crystal on the upper cover glass. In many cases it consisted of a single disclination domain with two parallel brushes extending most of the length of the domain. The arrows in *Figures 1j* and *k* indicate the same regions of the sample, the domains growing by both enlargement and merger. There is apparently a continuous film on the lower cover glass, the small domains being highly mobile (moving as a unit) during the early stages of polymerization. Merger of two single disclination domains resulted in only one disclination of the same type.

In the region corresponding to *Figure 1a*, similar domains are seen, of varying size; the ring is a region bridging the two slides (*Figure 1l*). ANA polymerized at 200°C developed similar structures[3]. Although most of the domains were black and white between crossed polars, a few of the domains in thicker regions, as at the upper right of *Figure 1l*, were brilliantly coloured. The black four-brush pattern is superimposed on a uniform colour; the origin of the colour, which does not change as the dimensions change due to the addition of other (small) domains, is at present unknown.

Seventeen hours later, still at 180°C, the material in the ring had polymerized, but the remainder of the material in the two areas had stayed nearly the same. The major difference after this time was that a number, but not all, of the single disclination domains, originally having a simple cross when observed between crossed polars, had developed a concentric ring pattern. This structure was retained as the sample was then cooled to room temperature (*Figures 1m* and *n*). For these two figures the cover glasses were split apart, the region shown corresponding to the material on the bottom cover glass; similar material was observed on the upper cover glass. The ring structure and four-brush patterns were unchanged if the sample was heated to 350°C, the maximum temperature for our hot stage.

As indicated above, ANA acted in a similar fashion when polymerized between slides. The sublimation/recrystallization occurred, however, at least 40°C higher in the absence of the *m*ABA. In addition, the final morphology was considerably different. Although simple, single-cross domains could be found in limited numbers in both the P(ONA/*m*OBA) and PONA samples, most of the domains in PONA transformed so as to have radial rather than concentric lines (*Figure 2*), suggesting that *m*ABA was still present in the presumed copolymer, despite its low melting point, and was affecting the morphology.

Figure 3 shows reflected (a, c, e) and polarized (b, d) light micrographs of the three types of morphologies observed in the thinner central regions of the samples used for d.s.c. and i.r. The small mounds in *Figure 3a* are seen to be single disclination domains in *Figure 3b*, with varying orientations. A number of the domains are totally black, except for a segmented bright rim. By reflected light they appear similar to those giving rise to the four-brush pattern; their morphology has not yet been identified by TEM. *Figures 3c* and *d* show larger disclination domains, with the rings clearly visible by reflected light. Also present are spherulite-like objects consisting of radiating fibrils; these have essentially no

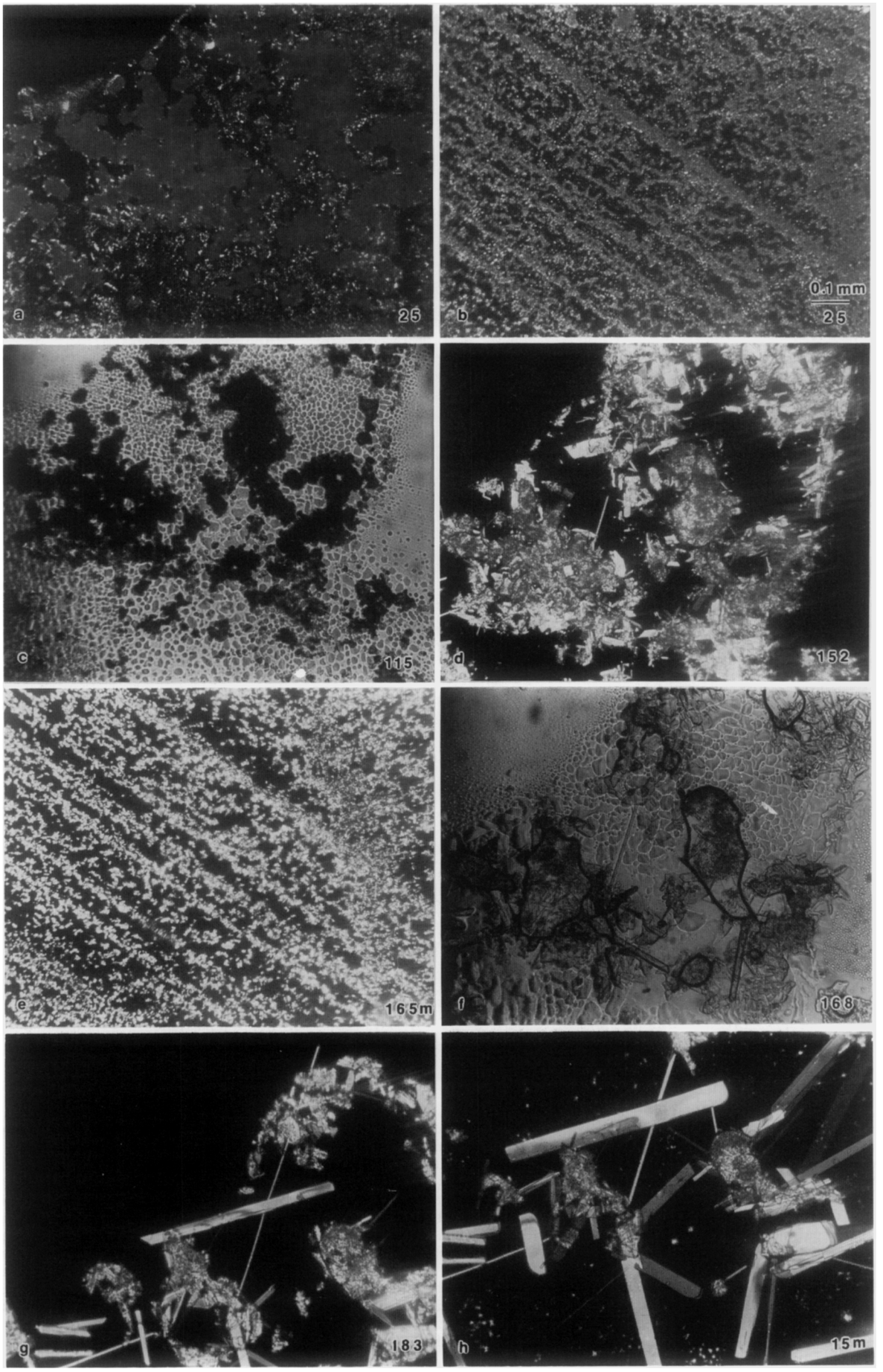
a
25
b
0.1 mm
25
c
115
d
152
e
165m
f
168
g
183
h
15m

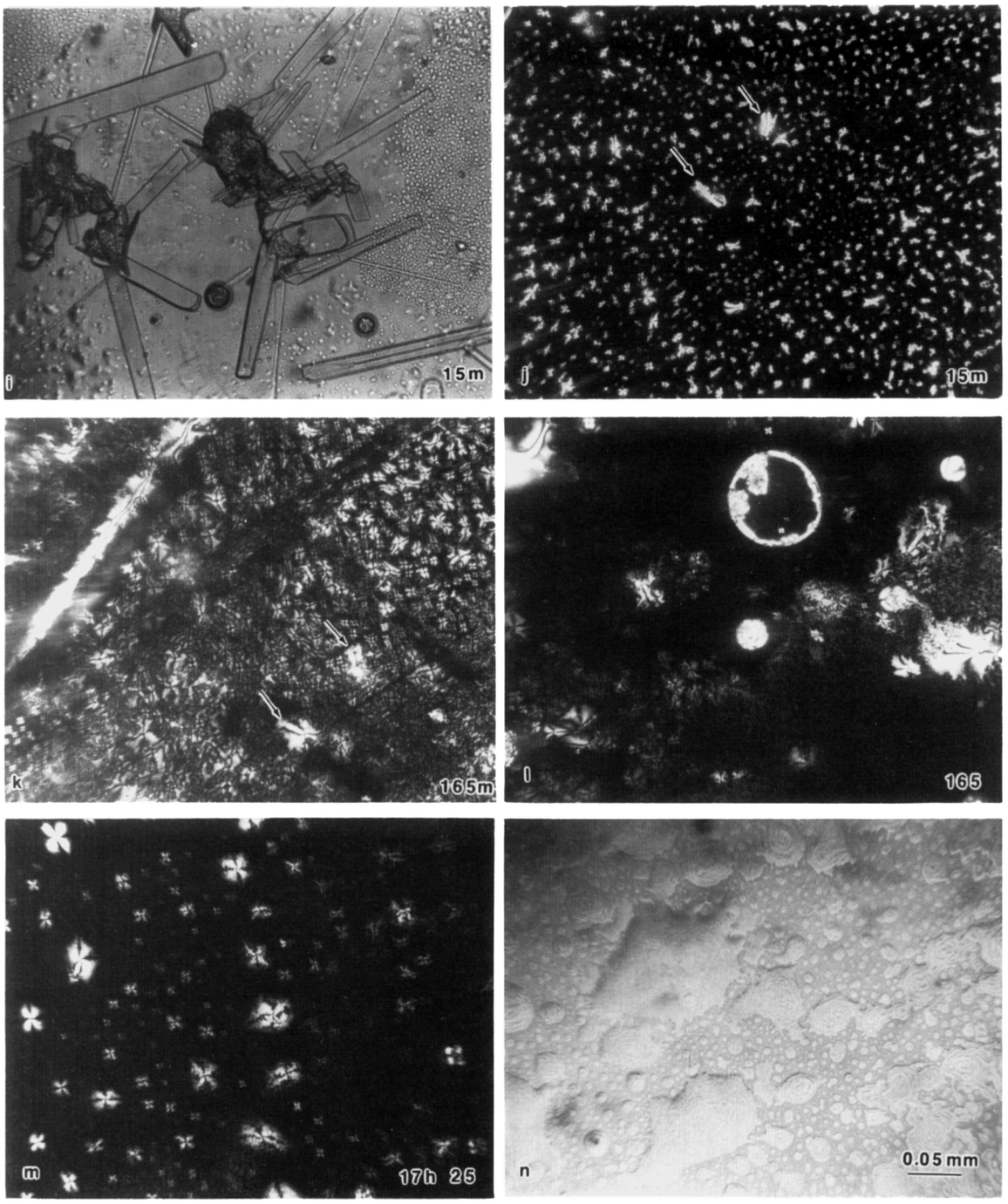

Figure 1 Optical micrographs, taken with crossed polars unless indicated, with labels indicating temperature (in °C, (a)–(g)) or time (in min) after reaching 183°C. All magnifications are the same, except (n). (a) Region I, as-cast 1/1 ANA/*m*ABA film at edge of film. (b) Region II, as-cast 1/1 ANA/*m*ABA film near centre of the film. (c) Region I at 115°C, transmitted light; the grey spots are molten. (d) Region I at 152°C; sublimation and recrystallization have occurred. (e) Region II at 165°C; sublimation–recrystallization and melting have occurred. (f) Region I at 168°C, transmitted light; the areas outlined with black lines are regions in which the molten material bridges the gap between the slides. (g) Region I at 183°C; some of the crystals in (d) and (f) have grown, others have melted. (h) Region I at 183°C, 15 min after (g), showing further sublimate crystal growth plus the initiation of polymerization. (i) Same as (h) in transmitted light partially shadowed (at left) with an aperture. The polymerized material consists of mounds in a uniform thickness molten film. (j) Region II, 15 min after reaching 183°C. Polymerization in small domains, each with a cross at its centre. Arrows indicate the same regions in (j) and (k). (k) Region II at 184°C, 165 min after reaching 183°C. Numerous single disclination domains can be seen. (l) Region I at 184°C, 165 min after (g). The circle with the bright ring is a 'bridge' region; only the outside has polymerized, whereas the smaller circular region below it has both polymerized and crystallized. Single disclination domains are in various areas, the region at upper left being outside the original cast film. (m) At room temperature, after 17 h at 183–184°C and separation of the cover slips. The four-brush pattern of the single disclination domains has been disturbed by a ring pattern. (n) Higher magnification, reflected light of a portion of the area in *Figure 1m*; irregular, circular ridges are visible

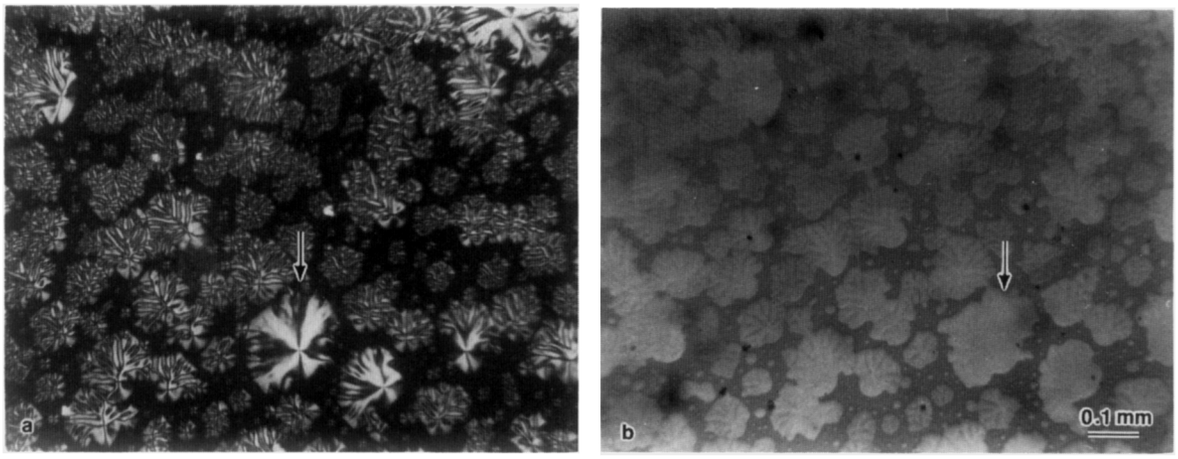

Figure 2 Optical micrograph of PONA constrained thin film samples polymerized at 200°C after cooling to room temperature. Arrows indicate identical domains. (a) The birefringent pattern observed in each 'domain' develops as the sample crystallizes during polymerization. (b) The domains with radical birefringence lines have radiating ridges; the remainder are smooth but are believed to be crystalline also

birefringence. The third type of structure is shown in *Figure 3e*; these domains of parallel striations also have essentially no birefringence. The different types of structures are found in different areas, with merger of the two types at boundaries between the regions. These variations may be due to differences in relative concentration of the two monomers (and the products of their reactions that have the lower T_ms); the films in these areas are of essentially the same thickness.

The thicker regions of the sample, on the two ends of the slides, consisted (*Figure 4*) of islands of material, apparently bridging the gap between the two slides, and diamond-shaped structures. The latter are seen to be birefringent (*Figure 4b*) and often extend out from the islands (*Figures 4a* and *c*, large-headed arrows); in *Figure 4b* the birefringence shows that they lie partially under the islands. These structures are multilamellar single crystals; the smaller-headed arrows in *Figures 4a* and *c* indicate small, nearly square single-lamella crystals (see next section). The birefringence is attributed to a common orientation of the carbonyl groups, e.d. (see below) showing that the molecular axes are parallel to the light beam.

Electron microscopy

Figures 5a and *b* are electron micrographs of regions from, respectively, the bottom and top cover slips of the sample in *Figure 1b*, i.e. an area near the centre of the original film. Rings of the same order of size as in the optical micrograph are seen on the large domain in *Figure 5b*, but they do not appear to be shadowed. Small spacing rings of high contrast are seen on the smaller domains. In some cases they appear to be the edges of lamellae; in other cases they are only ridges. The inset *hk*0 e.d. pattern is properly oriented with respect to the region underneath it. The pattern resembles that in *Figure 12d* but is more arced. At this time we cannot relate the molecular orientation (normal to the film) to the morphology, the morphology suggesting circumferential lamellae on edge which would give rise to a radially oriented fibre pattern.

Figure 6 is a replica of a region containing the domains of parallel striations. As in the case of *Figure 5*, ridges are seen, but the samples appear to be covered with a relatively structureless film. This sample was not washed with acetone before shadowing, but that does not appear to make a difference; the sample in *Figure 5* was washed. Further examination of the morphology of these structures and the origin of the contrast is in progress.

Figures 7a and *b* are fracture surfaces from a thick region of the P(ONA/*m*OBA) sample in *Figure 1*, presumably with a structure similar to the regions bridging the gap between the cover slips in *Figure 1l* or *Figure 4*. Narrowly spaced striations (200–300 Å spacing, inset and arrows) are seen in some regions of *Figure 7a*, radiating from a centre just above the centre of the micrograph. Assuming that these striations correspond to lamellae nearly normal to the surface, the centre would correspond to a disclination core. In the lower right of this figure and in *Figure 7b*, lamellae are seen which seem to be more or less parallel to the fracture surface. *Figure 7b* shows an area in the thick region in which most of the copolymer was removed with the other slide. Most of the lamellae are parallel to the surface. The inset *hk*0 e.d. pattern is phase I (see below). Its form suggests substantial common orientation over relatively large areas. *Figure 7c*, from the sample used for i.r. and d.s.c., is believed to be from a region similar to that shown in *Figure 4*, the material at the upper right being the diamond-shaped structures protruding out into the thin areas. They are seen to consist of multiple lamellae. In *Figures 7b* and *c* the lamellae parallel to the surface are about 100 Å thick.

As indicated by the transmission electron micrographs in *Figure 7*, a lamellar structure is seen, in some cases, for the P(ONA/*m*OBA) copolymer polymerized in constrained thin films. In addition, in some samples, well-formed, individual lamellar crystals can be found. Although, as shown in *Figure 4*, they are found associated with thick regions of the samples, in some cases they have also been observed in thinner samples. It is not yet known whether they always develop near the edge of the films as in *Figure 4*, suggesting a dependence on composition, or whether the particular polymerization conditions determine their formation.

Figures 8a–c are electron micrographs of the various types of lamellae observed in a thin film cover slip sample polymerized for 5 h at 180°C. The lath-like crystals, ~150 Å thick, are slightly thicker than the irregular edged lamellae, as shown by the thin edges where they 'merge'

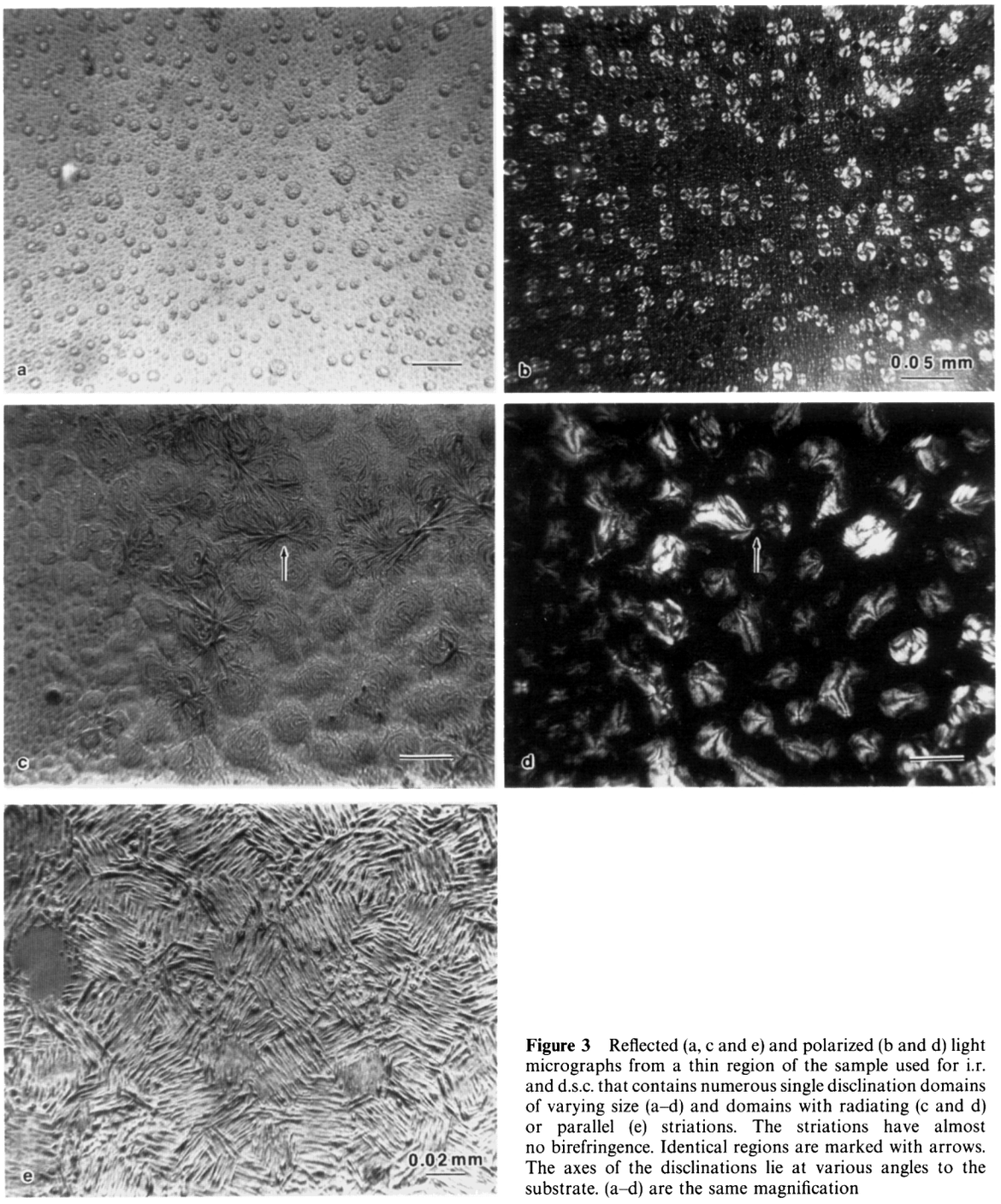

Figure 3 Reflected (a, c and e) and polarized (b and d) light micrographs from a thin region of the sample used for i.r. and d.s.c. that contains numerous single disclination domains of varying size (a–d) and domains with radiating (c and d) or parallel (e) striations. The striations have almost no birefringence. Identical regions are marked with arrows. The axes of the disclinations lie at various angles to the substrate. (a–d) are the same magnification

(*Figure 8a*). The laths and irregular edged lamellae appear to have grown independently for a time, i.e. in the melt rather than on the glass, overlapping in some regions (large-headed arrows). In other regions (small-headed arrows) they appear to be growing on the surface, growth stopping when they meet. The inset e.d. pattern and selected area, as discussed below, indicate a phase I type *hk*0 pattern, with *b* parallel to the lath axes. The lath-like crystals have not been observed by optical microscopy, possibly because of their small lateral dimension.

Whereas the lath-like crystals have only a slight surface texture, linear striations (valleys, possibly narrow cracks) lying parallel to the long edges of the lamellae, the irregular edged lamellae have a clear surface texture (*Figure 8b*). The short ridges creating this texture extend almost to the edges of the lamellae, the outer edges of the lamellae being smooth. The ridges divide the lamellae into sectors, lying parallel to the 'growth direction' of the edges. Sectors are rather unexpected in extended chain crystals, as presumably occur here; they have been observed, however, by Dorset[12] in paraffin crystals. In addition, cracks are seen, parallel to one of the diagonals, that extend across the sector boundaries. The cracks, similar to those observed in lamellae of P*p*OBA[1] and PONA[2,3], appear to be brittle, i.e. there do not appear to be fibres drawn across the cracks as would be expected if chain folding, as in polyethylene lamellae, were present.

Nearly square lamellae, also slightly thinner than the laths, were also found. It is this type of lamellae, but often larger and thicker (more lamellae), that are observed by

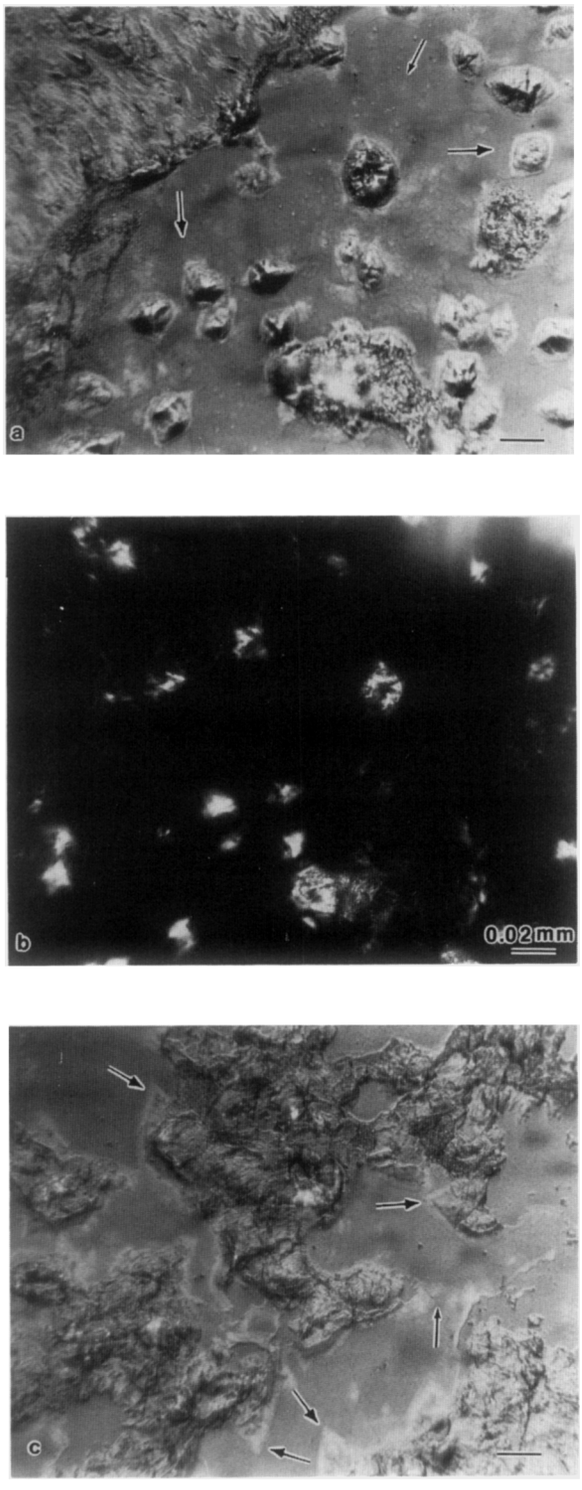

Figure 4 Reflected (a and c) and polarized (b) light micrograph of a thick area of the sample in *Figure 3*. Nearly square single-lamellar single crystals (small-headed arrows, see *Figures 6* and *8–10*) are visible in the thin areas between the thick regions. The large-headed arrows indicate multilamellar single crystals in between and partially underneath the thick areas

reflected light in *Figure 4*. In the preparation used for *Figures 8a* and *b* they were lying on top of the irregular edged lamellae (*Figure 8c*), whereas in a second, presumably identical, preparation they could be found isolated (*Figures 9a* and *b*). In both samples the corners are rounded and in *Figure 9*, in particular, the edges are somewhat irregular. Again, there is evidence of a slight degree of further growth of the square lamellae, which are about 100 Å thick, after overlapping the laths (small-headed arrows) or, as at the right of *Figure 9a*, considerable growth of the basal lamellae after overlapping each other (large-headed arrow). The

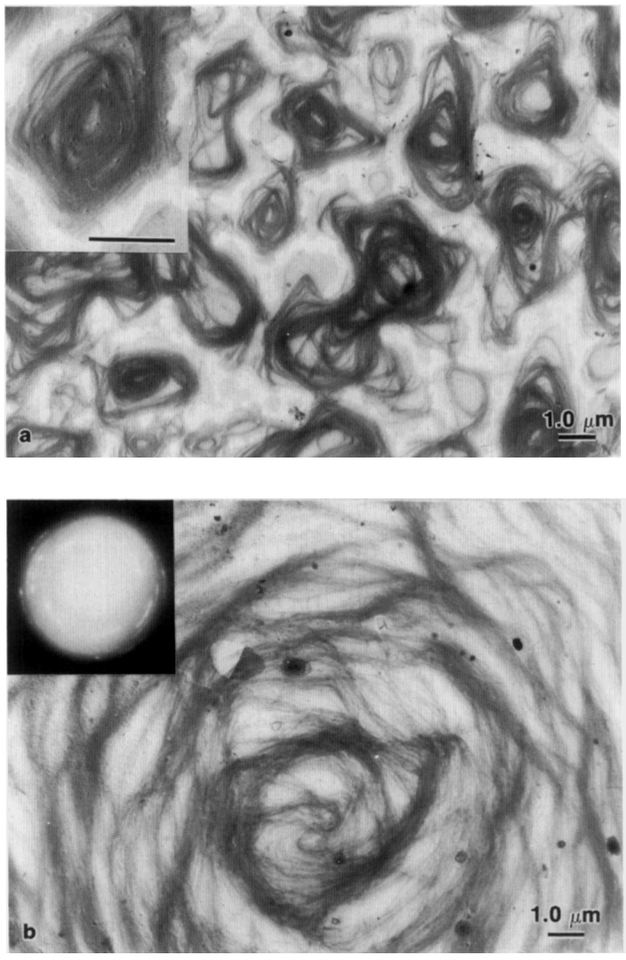

Figure 5 Transmission electron micrographs (sample floated on HF) of regions on (a) the top and (b) the bottom of the cover slips used for *Figure 1*. An enlargement of the central region of (a) is inset. In (b) a portion of the shadowing is peeled back near the centre. An e.d. pattern of a similar area is inset. Despite the high contrast, the surfaces of the domains are nearly featureless

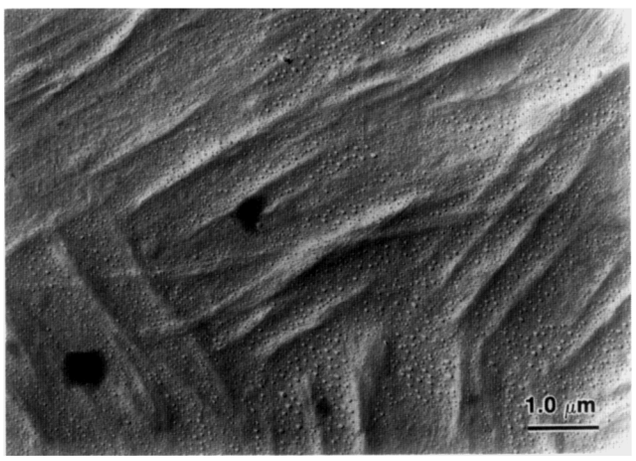

Figure 6 TEM micrograph of a replica from the region shown in *Figure 3e*

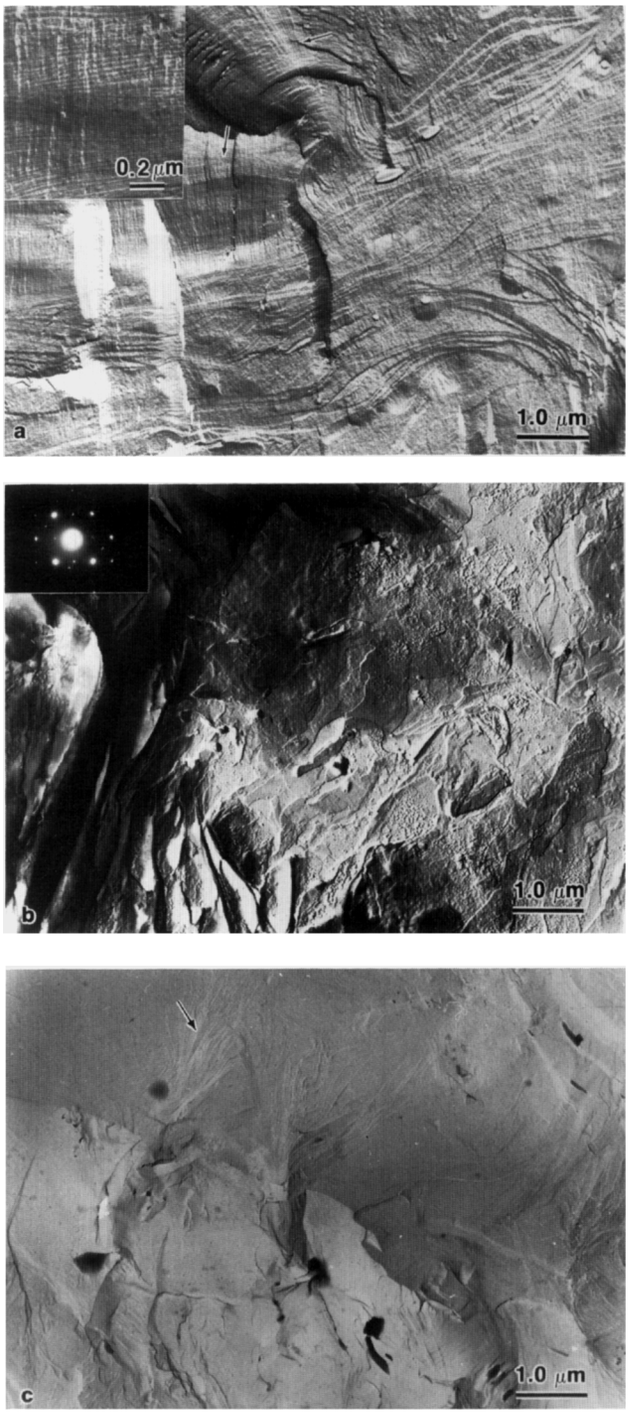

Figure 7 Replicas of fracture surfaces from a 'thick' 1/1 P(ONA/*m*OBA) sample similar to those used for the i.r. and d.s.c. samples. This material bridges the gap between the slides as it is polymerized. An enlargement of the striated region at centre left is inset in (a), an e.d. pattern (different area) in (b). The entire darker grey area designated by the arrow in (c) is believed to be part of one of the large 'square' crystals in *Figure 4*

lath-like lamellae in this preparation are seen to sometimes merge, as if growing on the substrate, and, in other cases, overlap, as if growing in the melt and being 'deposited' on top of each other.

Surprisingly, assuming these crystals grow by monomer or oligomer addition and polymerization primarily on the lateral faces, the square lamellae in the second preparation all show evidence of a primary nucleus, a bump at the centre that is often elongated at a slight angle to one of the diagonals, and a small surrounding more or less square region that is slightly thicker than the remainder of the lamella. In addition, very shallow undulations are seen on the surface forming rows parallel to one of the diagonals (and the long axes of the lath-like crystals). Possibly these are the forerunners of the cracks seen in larger crystals. A similar nucleus can also be seen on most of the irregular edged lamellae in the first

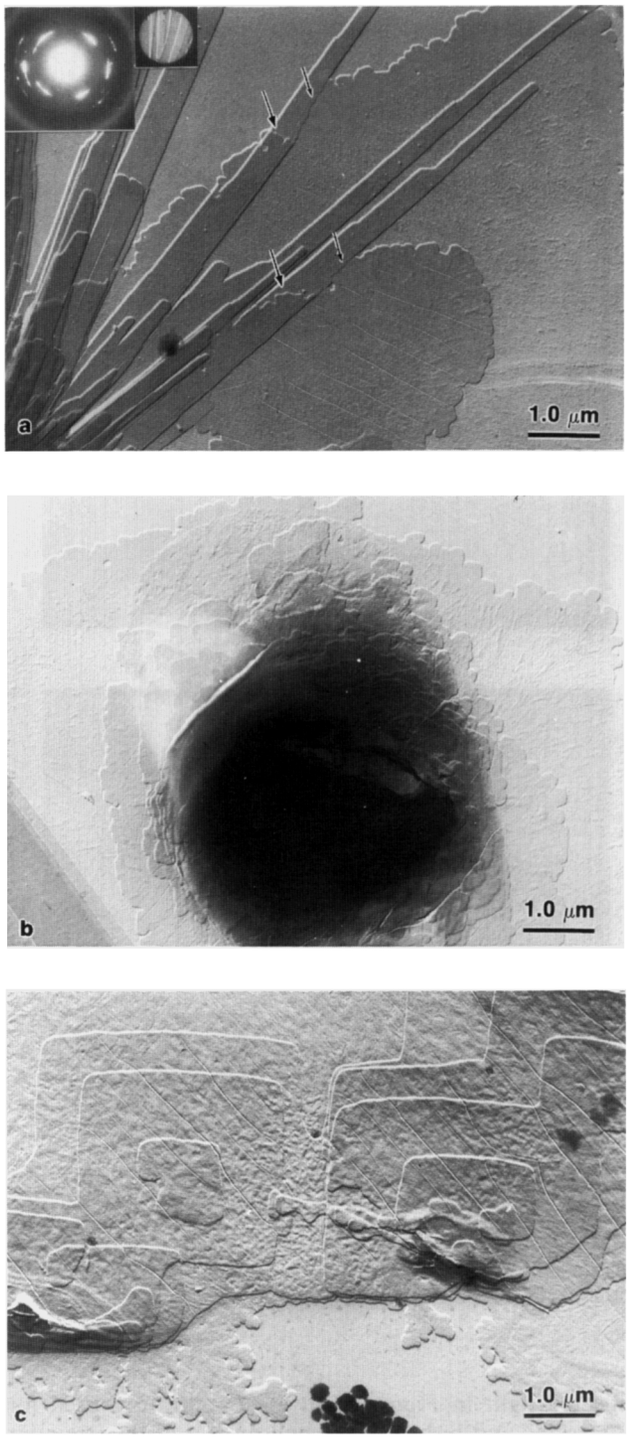

Figure 8 P(ONA/*m*OBA) 1/1 polymerized for 5 h at 180°C. (a) Lath-like crystals and overlapping (large-headed arrows) or merged (small-headed arrows) irregular edged lamellae. An e.d. pattern with its selected area is inset. (b) Irregular lamellae, presumably from a disclination domain, with a surface texture. (c) Nearly square lamellae on top of an irregular edged lamella

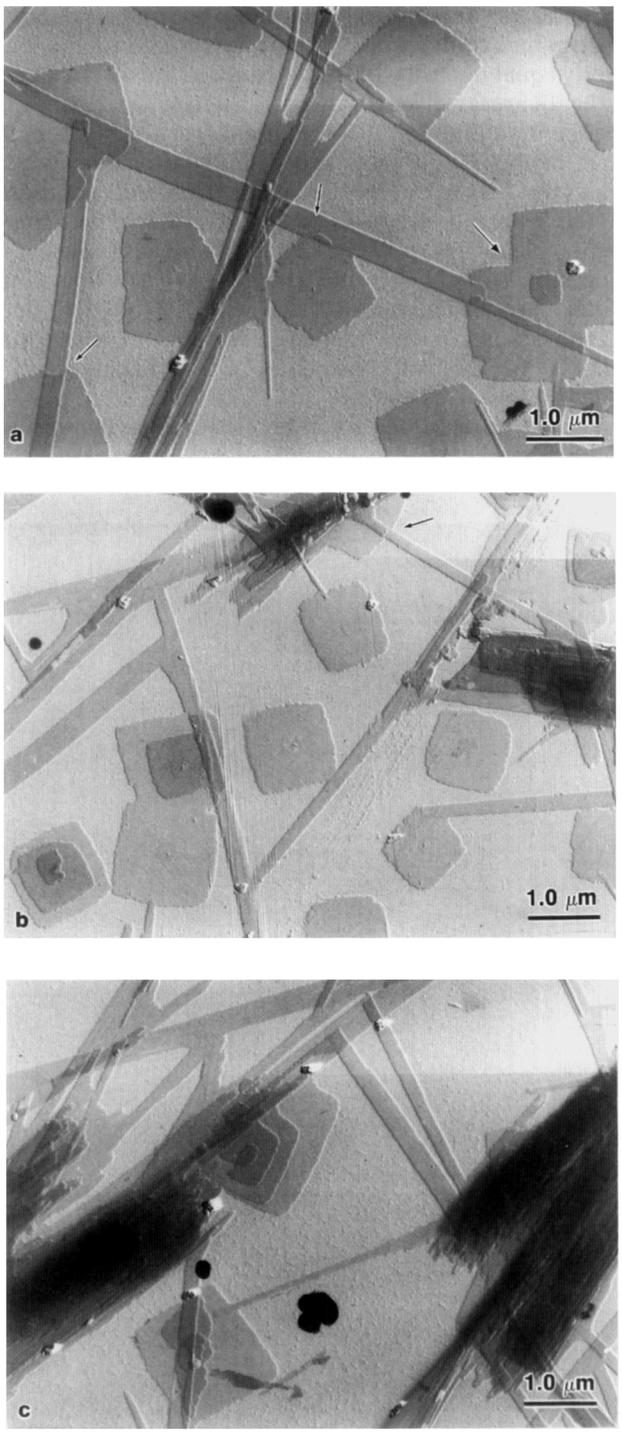

Figure 9 Micrographs of lamellae in another P(ONA/*m*OBA) 1/1 sample polymerized for 5 h at 180°C. Small-headed arrows represent regions of further growth of the square lamellae after overlapping the lath-like crystals, while the large-headed arrow in (a) indicates a region where two square lamellae overlap. Primary nuclei can be seen in the centre of most of the square lamellae. The thicker regions in (c) appear to be composed of lath-like crystals

preparation. The small cubic crystals seen in some of the micrographs are residue resulting from the HF attack on the glass.

Figure 10a shows a portion of a square-type lamella in a sample polymerized for 24 h at 180°C. The lamellae are somewhat more perfect, and appear larger than those polymerized for the shorter time; they still have rounded corners and slightly irregular edges. They are about 100 Å thick, the same as those polymerized for only 5 h. The lath-like lamellae were also present in this sample, but the irregular edged lamellae were absent. It is suggested that the latter develop into the square lamellae as they 'become more perfect'. For comparison, the lamellae in a PONA sample polymerized under similar conditions are shown in *Figure 10b*. The lamellae are much more rounded and irregular. Lath-like lamellae have also been seen, but they also differ from those seen for the copolymer. The morphology of PONA is discussed further in refs 2 and 3.

Figure 11 is a 110 dark field micrograph of a region

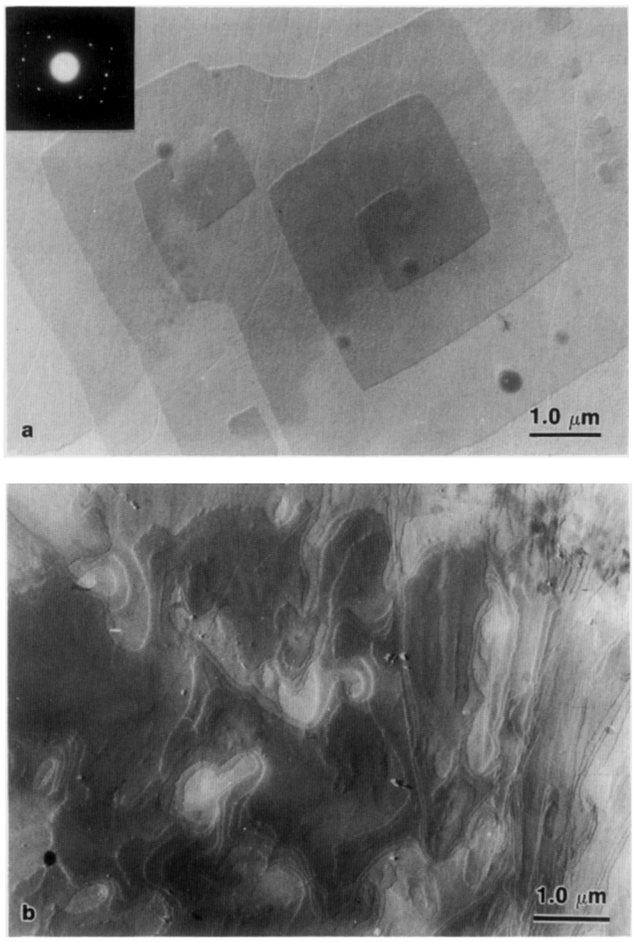

Figure 10 Lamellae in (a) a P(ONA/*m*OBA) 1/1 sample polymerized at 180°C for 24 h and (b) a PONA sample polymerized at 180°C for 14 h corresponding to a thin region of the sample in *Figure 2*. An e.d. pattern is inset at the proper orientation in (a)

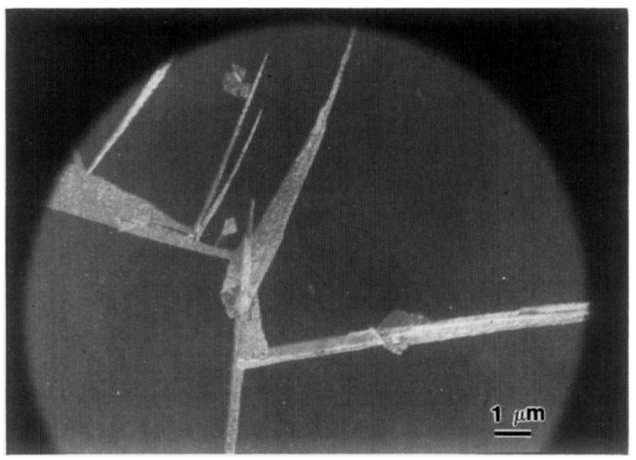

Figure 11 Dark field (110) electron micrograph of the lath-like crystals

of the 180°C, 5 h sample containing lath-like crystals. As in dark field micrographs of folded chain crystals of flexible backbone polymers, the entire crystals do not 'light up'. The patchiness of the diffracting regions here suggests regions of varying order within the crystal, not just a waviness of the substrate. Dark field micrographs of the square and irregular edged lamellae have not yet been obtained.

Electron diffraction

Figures 12a and *b* are representative e.d. patterns from the lath-like (a) and square and irregular edged lamellae (b). The spacings are identical, but the lattice for the square and irregular edged lamellae appears to have 'extra' reflections. The long axis of the laths corresponds to the *b* axis; the patterns contain weak, but nearly equal intensity 100 and 010 reflections. The cracks in the square lamellae are also parallel to *b*. These patterns also contain 100 and 010 reflections, relatively stronger than for the lath patterns and with 010 usually stronger than 100. The 'extra' reflections in *Figure 12b* are those on the $h\frac{1}{2}0$, ($2\frac{1}{2}0$, $3\frac{1}{2}0$, $4\frac{1}{2}0$), $h\frac{3}{2}0$ ($1\frac{3}{2}0$, $3\frac{3}{2}0$, $4\frac{3}{2}0$ with very weak $0\frac{3}{2}0$ and $2\frac{3}{2}0$) and $h\frac{5}{2}0$ ($2\frac{5}{2}0$, $3\frac{5}{2}0$ and $4\frac{5}{2}0$) row lines, suggesting a doubling of the lattice in the *b* axis direction. Streaks are also seen associated with the 100, 010 and 020 reflections. Weak 'satellite' reflections are seen for a number of the *hk*0 reflections, at a spacing of $\frac{1}{3}a$ (*Figures 12b–d*, arrows).

The lattice spacings for both patterns, assuming an

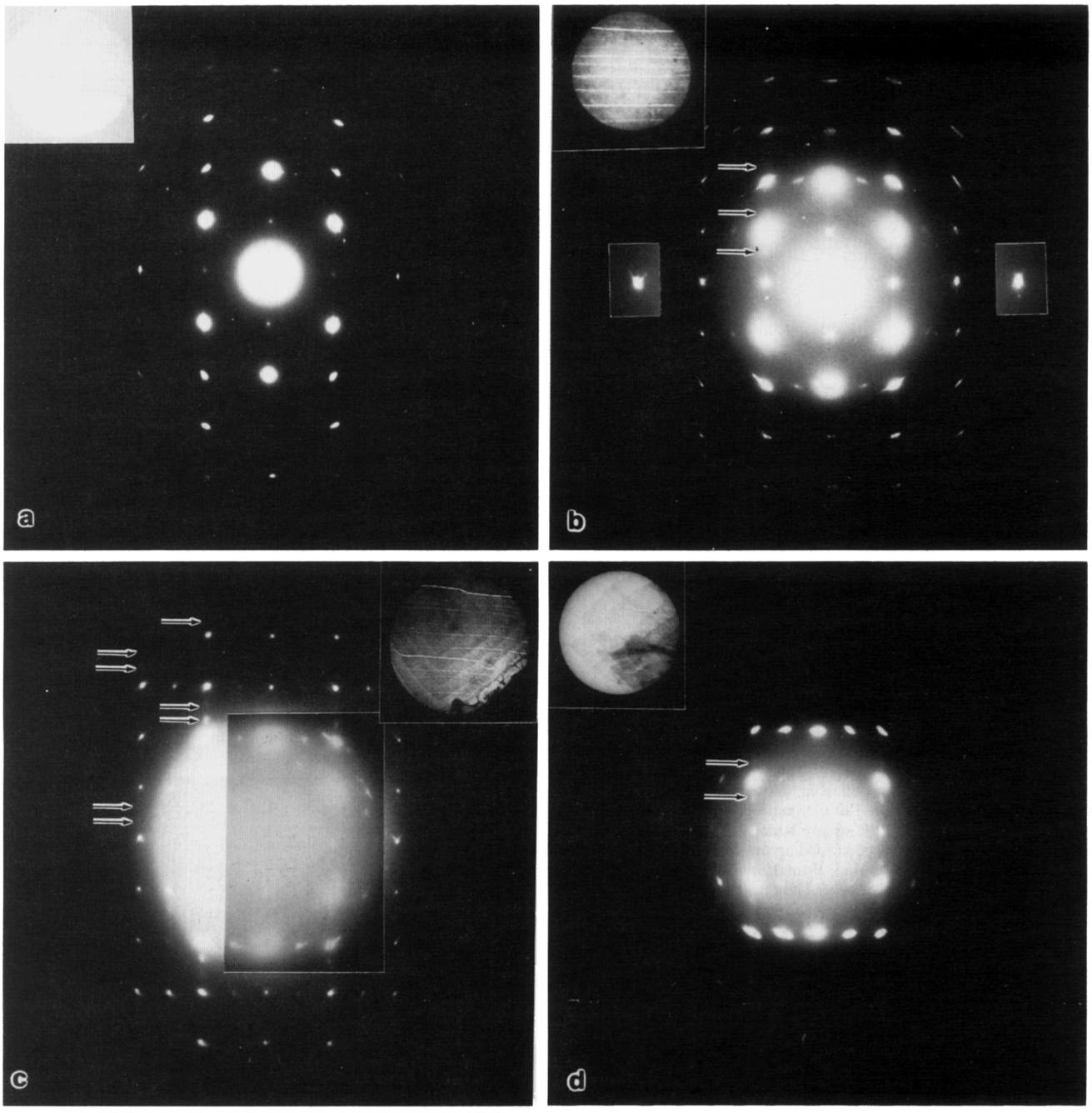

Figure 12 E.d. patterns (and selected areas) of P(ONA/*m*OBA) 1/1 polymerized at 180°C for (a) 5 h and (b), (c) and (d) 23 h. The pattern in (a) is from a lath-like crystal, those in (b)–(d) from square crystals. In (b)–(d) the satellite reflections are indicated by arrows. Enlarged images of 020 are inset in (b)

orthorhombic unit cell, are $a=3.8$ Å, $b=4.7$ Å (with b doubled in *Figures 12b–d*). The pattern from the lath resembles that of phase I in P*p*OBA and PONA, for which the corresponding spacings for phase I are 3.8 and 4.6 Å (ref. 1) and 3.8 and 4.8 Å (ref. 2), respectively; homopolymer P*m*OBA has $a=3.7$ Å, $b=4.5$ Å (refs 4–7), all in projection on the a^*b^* plane. Phase I for PONA is monoclinic[2]. A similar doubling of the lattice has been observed for PONA, the intensity of the 'extra' reflections varying, as here, from crystal to crystal (*Figures 12c, d*)[2]; some, but not all, of the 'extra' reflections are strong in phase II P*p*OBA or PONA patterns[1,2].

Considering the similarity in these *hk*0 diffraction patterns and the low melting point of *m*ABA, possibly permitting it to escape from between the slides below the polymerization temperature, an obvious concern is whether or not the 1/1 samples actually have that composition or are, possibly, PONA. Differences and similarities with related observations for PONA are described in the remaining sections. In terms of lamellar morphology, however, we have never observed lamellar crystals of this degree of morphological 'perfection' for PONA polymerized in a similar manner. Lath-like crystals with tapered edges and rounded lamellae in thicker regions are observed (*Figure 10b*, see also refs 2 and 3). In addition, the disclination domains, after crystallization, have a distinctly different morphology (*Figures 1m, n* compared to *Figures 2a, b*).

3/1 and 1/3 copolymer

A limited number of observations have been made of a 3/1 P(ONA)/*m*OBA sample polymerized at 180°C for 5 h. The micrographs and diffraction patterns are almost identical to those shown for the 1/1 sample above, lath-like, irregular edged and square lamellae being seen (*Figures 13a* and *b*). The 1/3 sample yielded only regions with irregular surface striations (*Figure 13c*), resembling those in *Figures 5* and *6*. E.d. patterns could not be obtained from the 1/3 sample. Optical micrographs during polymerization of these samples have not yet been obtained.

Only a limited amount of research has been done to date on the effect of higher temperatures of polymerization and annealing. *Figure 13d* is from a 3/1 P(ONA/*m*OBA) sample polymerized for 3 h at 250°C and then annealed at 300°C for 15 min. The morphology resembles that of the 'superlattice structures' observed in 3/1, 1/1 and 1/3 P(ONA/*p*OBA) polymerized at 180°C for various periods of time[7]. The relationship of this structure to the lamellae is still being sought. It has, to date, only been seen in copolymer samples and appears to grow on or from single crystal lamellae lying on the substrate.

Sheared samples

As shown for P(*p*OBA/ONA) (e.g. refs 13–16), shearing or drawing of solution or bulk polymerized liquid crystal copolymer samples generally yields samples that give

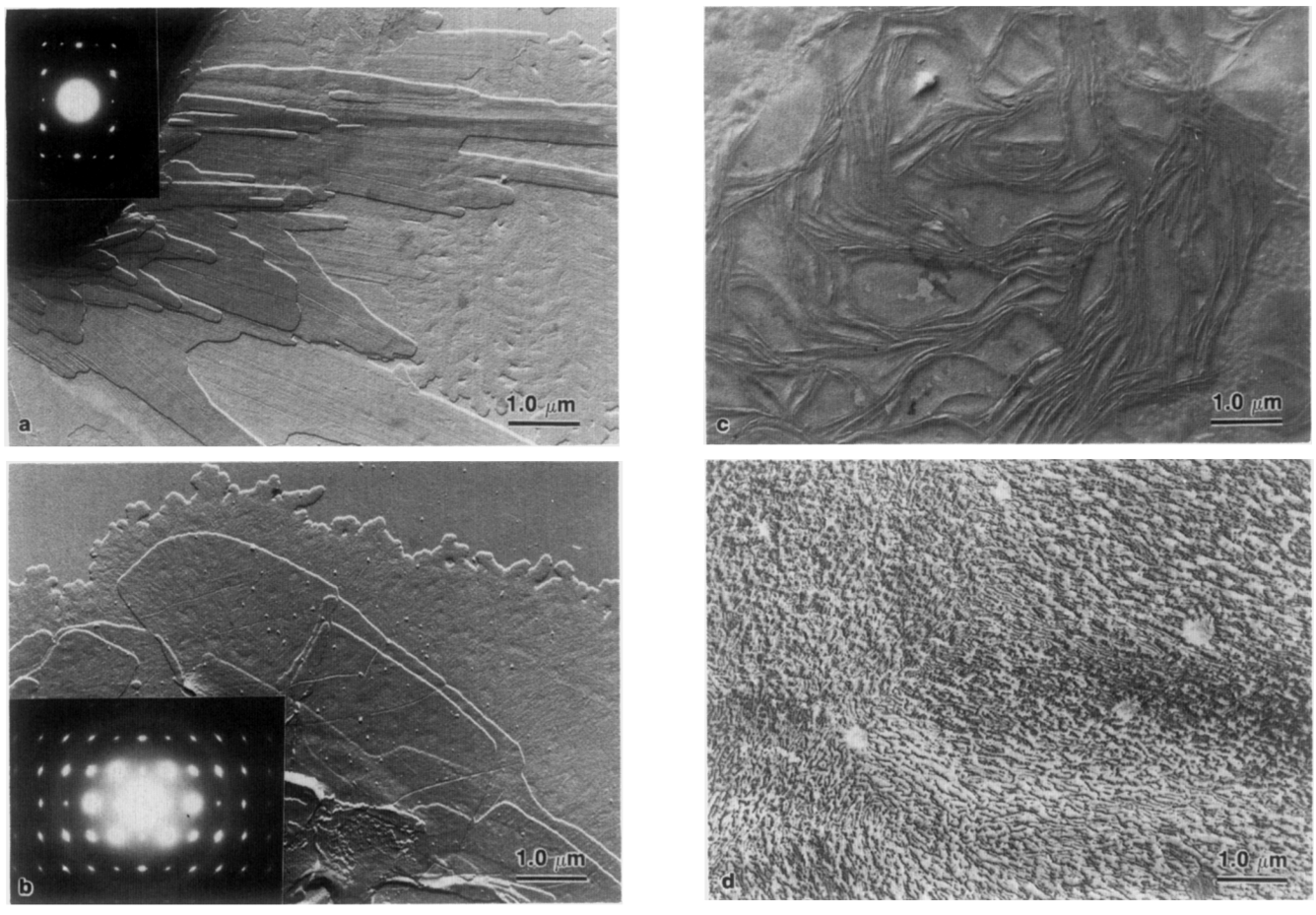

Figure 13 Electron micrographs of P(ONA/*m*OBA) 3/1 (a, b) and 1/3 (c) polymerized at 180°C for 5 h. The lath-like lamellae in (a) extend out from a disclination domain. E.d. patterns are inset; the pattern in (b) is rotated by ~90°; (d) is the 3/1 copolymer polymerized at 250°C for 3 h and then annealed at 300°C for 15 min

X-ray or e.d. fibre patterns with non-periodic lattice (n.p.l.) spacings in the fibre axis direction; the spacing of the innermost of these reflections is linearly related to the average composition in the regions giving rise to the diffraction. Thus, PONA has a 8.3 Å spacing, P*p*OBA a 6.1 Å spacing and 1/1 P(*p*OBA/ONA) a 7.2 Å spacing. All also have ~2.1 Å meridional reflection corresponding to the average separation of non-adjacent atoms (e.g. C–C–C or C–C–O) bond distances in the *c* axis direction, this being 008 in PONA and 006 in P*p*OBA. We have confirmed these results[4–7] and obtained a similar linear relationship for copolymers of OBBA with ONA[4–7,17]. Thus, in those polymers, one can use the sheared e.d. patterns to determine local composition. However, e.d. patterns of P(*m*OBA/ONA) samples sheared at 190 or 200°C generally have only the 2.1 Å meridional reflection, although several equatorial and one quadrant reflections can be observed (*Figure 14a*). Only in one sample sheared at 200°C was an 'inner' meridional reflection observed at 6.8 Å from a 1-chloronaphthalene polymerized sample, suggesting an n.p.l.-type pattern. The 2.1 Å reflection in *Figure 14a* appears doubled, with the additional reflection

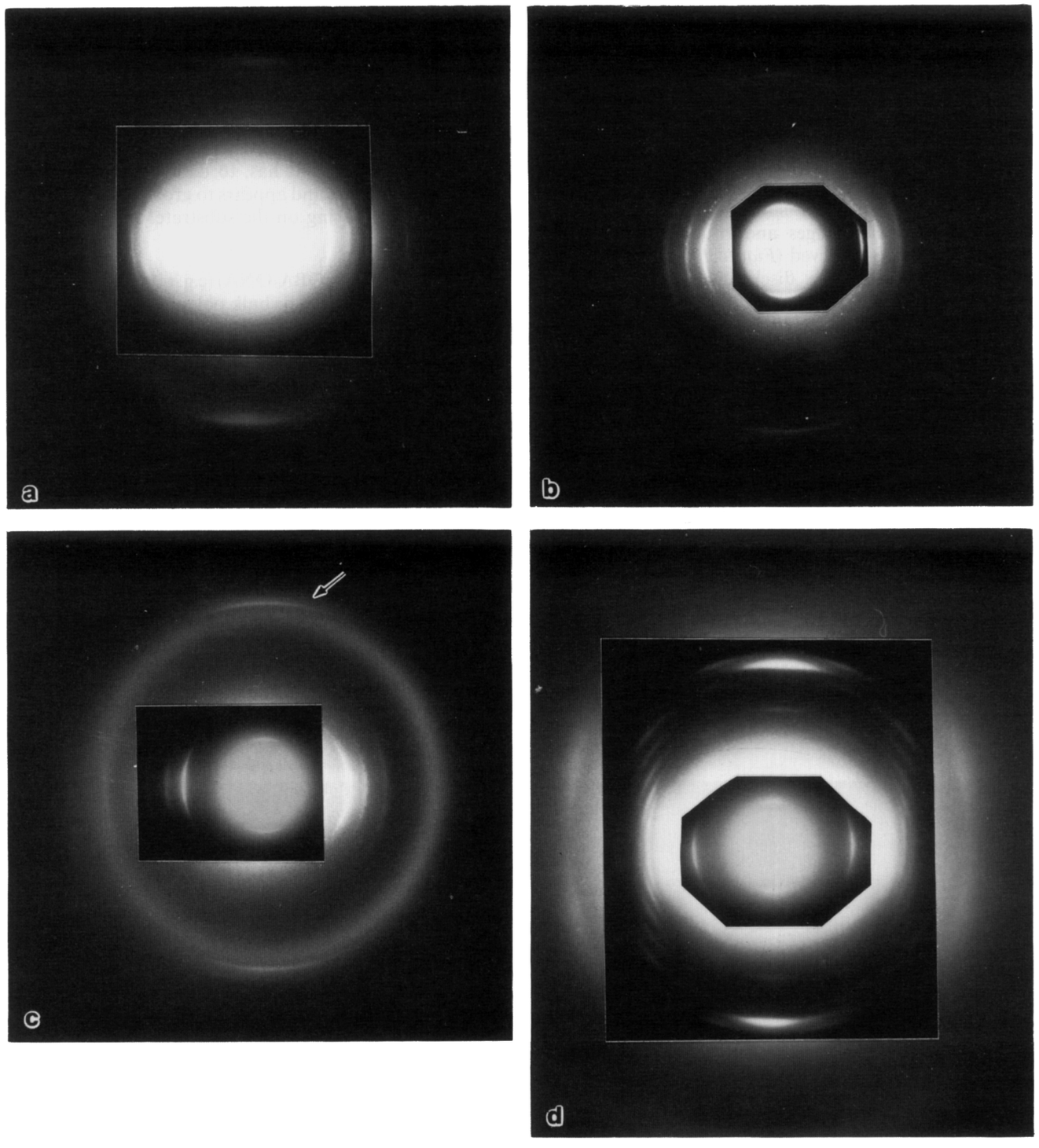

Figure 14 E.d. patterns from sheared P(ONA/*m*OBA) 1/1 samples. (a) and (b) were polymerized at 180°C for 5 h before shearing; (c) was polymerized in 1-chloronaphthalene. (a) Sheared at 200°C; (b) sheared at 220°C, annealed at 180°C for 6 h; (c) sheared at 300°C, annealed at 250°C for 16 h. An arrow indicates the 102 reflection. (d) PONA polymerized at 200°C for 5 h and sheared at 280°C

being at a smaller angle. This was seen fairly frequently with a variation in relative intensity of the two reflections and may be due to two different projections of the C–C–C type distances on the *c* axis.

Shearing at 250 or 300°C, however, yields patterns similar to those obtained by annealing (*Figures 14b, c*). *Figures 14b* and *c* are e.d. patterns of a melt polymerized sample (180°C, 5 h) that was scraped from the glass, sheared at 220°C and annealed at 180°C for 6 h (*Figure 14b*) and a solution polymerized sample sheared at 300°C and annealed at 270°C for 24 h (*Figure 14c*). The meridional spacings in both are 8.25 and 2.1 Å, i.e. they approximately correspond to the 002 and 008 reflections of sheared solution and melt polymerized PONA, although 002 appears to be ~0.1 Å shorter. Only a single 2.1 Å reflection was seen in all of these samples, with 102 quadrant reflections also frequently observed (arrow in *Figure 14c*). Sheared, annealed 3/1 copolymer yields similar patterns. On the other hand, in PONA, 006 and numerous equatorial and quadrant reflections can often be seen (*Figure 14d*), which are not present in any of the copolymer samples we have examined. It is also noted that the sheared copolymer and PONA patterns differ from the monoclinic PONA whisker patterns ($\beta = 87°$, ref. 2) in which the c^* axis is at an angle to the shear direction; this is attributed to the fibre (rotation crystal) nature of the sheared patterns and some variation in orientation leading to arcs rather than spots. Usually, only three equatorial reflections can be seen (as occurs also for most sheared PONA samples); they correspond to 110, 200 and 210 of the *hk*0 patterns; occasionally, as in *Figure 14a*, 220 can also be seen (outside the insert). The lack of all meridional reflections, except the 2.1 Å reflection, and the diffuseness of the equatorial reflections suggests considerable disorder in the packing of the as-sheared samples; transesterification during high temperature shearing and/or annealing may result in blocks of ONA.

Thermal analysis

By scraping the material similar to that in *Figure 4* from the slides with a razor blade, it was possible to obtain sufficient material for d.s.c. scans. Typical scans at 50°C min^{-1} of 1/1 copolymer and PONA samples melt polymerized at 180°C for 23 h are shown in *Figure 15*. In the copolymer a peak is seen at 282°C while in PONA the peak is at 320°C and has a higher heat of transition. Also shown is a scan of the copolymer polymerized for 40 h at 180°C; the maximum is at 291°C. The 3/1 P(ONA/*m*OBA) sample had a peak at 284°C (23 h) or 292°C (40 h) while the 1/3 sample (23 h) had a very broad peak centred at about 260°C. The high-temperature peak at 411°C, seen in the PONA scan, is not seen in the copolymer scans. This also occurs for P(*p*OBA/ONA) copolymers (e.g. ref. 9). The rise in the 23 h polymerized copolymer plot at elevated temperature is attributed to further polymerization.

Solution polymerized (in 1-chloronaphthalene at 235°C for 22 h) 1/1 copolymer material shows a sharp peak at 150°C, and a broad, shallow peak at about 230°C, suggesting a difference in configuration between the melt and solution polymerized sample. *FT*i.r. scans of the solution polymerized material were, however, identical to those of the melt polymerized material (see *Figure 16*). The 150°C peak moves up in temperature with annealing, remaining about 30°C above the annealing temperature for 20–30 h annealing time, whereas the 230°C peak does

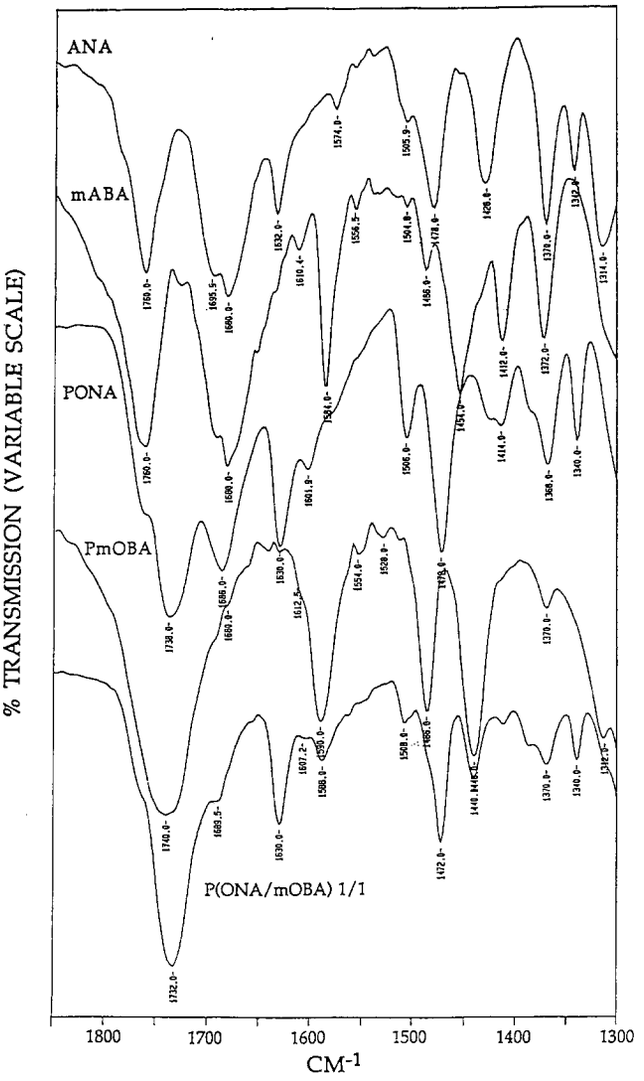

Figure 16 *FT*i.r. scans of the monomers (*m*ABA and ANA), homopolymers (P*m*OBA and PONA) and copolymer (1/1). See text for details of polymerization

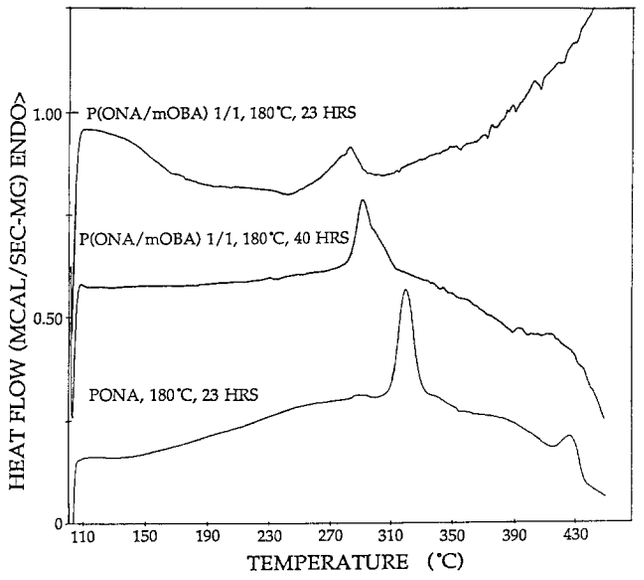

Figure 15 D.s.c. scans at 50°C min^{-1} of P(ONA/*m*OBA) 1/1 and PONA samples polymerized at 180°C for 23 h and 40 h (copolymer). All scans are normalized to 1 mg

not change for low annealing temperatures. Annealing at 230°C for 20 h resulted in large peaks at 310 and 345°C. It is noted that 1/1 P(*p*OBA/ONA) polymerized in Therminol 66[4–7,18] and 1-chloronaphthalene[19] has a small peak at around 245°C and no peak, respectively; annealing both types of samples results in peaks at temperatures above the annealing temperature.

Infra-red spectroscopy

*FT*i.r. scans were obtained from the thick film samples in order to at least qualitatively evaluate the degree of polymerization from the replacement of C=O stretch carboxy and acetoxy bands with an ester band, and the relative composition. *Figure 16* shows i.r. scans in the 1850–1300 cm^{-1} region for the monomers, homopolymers (PONA, 200°C, 22 h; P*m*OBA, 1-chloronaphthalene, 235°C, 4 h) and copolymer (1/1, 180°C, 7 h). The 1760 cm^{-1} acetoxy band is almost completely missing and the 1680, 1695 cm^{-1} carboxy bands are also greatly diminished in all of the polymers. On the other hand, the 1736 cm^{-1} ester band has developed. The results suggest a higher molecular weight for the copolymer than either of the homopolymers shown.

The bands at 1584 and 1486 cm^{-1} and at 1630, 1472 and 1340 cm^{-1} can be attributed to the *meta*-substituted benzene and naphthalene residues, respectively. All are seen to be present in the product, indicating that it is a copolymer or, at least, a blend of the two homopolymers.

DISCUSSION AND SUMMARY

The primary concern is whether or not we are dealing with P(ONA/*m*OBA) copolymer or homopolymer PONA, and, if copolymer, its composition and configuration. The fact that polymerization was conducted above the T_m of *m*ABA (135°C) but below the T_m of ANA (226°C) suggests that *m*ABA may have escaped from between the slides and we are dealing with homopolymer PONA. The relatively small difference in $T_{k\text{-}m}$ transition temperatures for thin film polymerized PONA and the 1/1 and 3/1 copolymers would tend to support this suggestion, particularly since the solution polymerized copolymer (from which the monomer might also have evaporated prior to polymerization) has a considerably different d.s.c. scan. The *hk*0 e.d. patterns are similar to those of homopolymer PONA, but are also similar to phase I P*p*OBA, P*m*OBA, P*o*OBA and POBBA patterns. The e.d. patterns from the sheared copolymer samples after annealing are also similar in *c* axis spacings to those of PONA, although the innermost reflection appears to have a slightly smaller (0.1 Å) spacing than 008 of PONA. The sheared PONA, for equivalent thermal treatment, appears to have better crystals.

On the other hand, the square crystals have not been observed for PONA; instead, large, multilayered, rounded edge lamellae are seen. The lath-like crystals in the samples here also differ from the lath-like crystals that have been observed in PONA[3]. Furthermore, the morphology of the single disclination domains, after crystallization, differs significantly from those of PONA and the striated domains have not been observed for PONA.

The i.r. scans, in particular, confirm the presence of both monomers in the polymerized material, at a ratio near that of the feed, in the thick regions of the samples (as used for *Figure 4*). Although this could possibly be due to a blend of homopolymer P*m*OBA and PONA, there is no evidence for P*m*OBA. Thus, we conclude that we have P(*m*OBA/ONA). The perfection of the lamellar crystals suggests that they might consist of alternating copolymer, permitting the apparently high crystallinity. Regrettably, however, we have not yet been able to isolate the various morphological structures to permit characterization of even their composition, let alone configuration. This high degree of order is destroyed by shearing; this occurs in all of the liquid crystal polymers we have examined. The similarity of the e.d. patterns from the sheared samples, after annealing, to those of PONA may be the result of transesterification reactions leading to blocks of homopolymer PONA; the effects of annealing both sheared and non-sheared samples is still under investigation.

The optical microscopy observations would be in agreement with the suggestion that copolymer was prepared, the monomers subliming, recrystallizing, melting and then polymerizing isothermally at temperatures below the T_m of ANA. Similar effects have been observed for pure *p*ABA[1], ANA[2,3], 4-acetoxy-4′-carboxy biphenyl[17] and mixtures thereof[4–7,17] all at temperatures well below the d.s.c. measured melting points. The only difference here is that the polymerizations were carried out above the T_m of *m*ABA. The sublimation and melting, however, occurred as low as 110°C. It is believed that the sublimate crystals in the copolymerization experiments are individual crystals of the two components, the *m*ABA crystals forming and melting (at about 124°C) before the ANA crystals form. The lower sublimation temperature for the ANA here than in pure ANA suggests some form of interaction. For pure *p*ABA and ANA the sublimate crystals have been shown to still be monomer[3,11]. The melt, however, differs. D.s.c. shows it to have a lower melting point and i.r. suggests a small degree of 'polymerization', i.e. it may be dimer or short chain oligomers or, more likely, related chemical species. The nature of the solution polymerized material is still being examined.

As pointed out in the Results section, the lamellae in the 5 h samples have the appearance of having initially been formed in the melt, depositing on the subtrate and then continuing to grow to some extent. This would agree with the optical microscopy observations, the single disclination domains, when small, being highly mobile in the surrounding melt, merging at times to form larger domains. As in the case of P*p*OBA[1], we propose that the lamellae and the single disclination domains grow in the liquid crystal state from the molten oligomer; in the case of the domains, crystallization occurs isothermally as the $T_{k\text{-}m}$ temperature reaches the polymerization temperature. This is accompanied by the transformation of the simple four-brush pattern to the ringed pattern. The single crystals and the lamellae in the thick regions may also grow as liquid crystal domains, transforming to crystalline domains as polymerization continues; the cracks would then correspond to shrinkage cracks resulting from the transformation. For P*p*OBA the phase I (HT) (the orthorhombic (pseudohexagonal) phase resulting when P*p*OBA phase I crystals are heated above $T_{k\text{-}m}$) to phase I transformation we have proposed[20]

involves shrinkage along *a*, thus resulting in the cracks along *b*.

Of particular interest relative to lamellar crystallization of polymers in general are our observations of a lamellar morphology and, for this polymer, the primary nuclei in the centre of the square and irregular lamellae. Lamellae on the order of 100 Å in thickness are characteristic of all of the liquid crystal polymers we have polymerized by the constrained thin film method. Since these are presumably extended chain crystals, growing by simultaneous polymerization–crystallization (in the liquid crystal state), the kinetic theory, as developed by Lauritzen and Hoffman[21] for folded chain crystals, would not seem to be directly applicable. On the other hand, the observable presence of the primary nuclei suggests a related mechanism. Although for P*p*OBA and here, the lamellar thickness appears to be independent of polymerization time and temperature, further studies of this effect are clearly warranted. In particular, for instance, the lamellae parallel to the substrate in *Figures 7b* and *c* are about 100 Å thick, similar to those in the square and lath-like single crystals, whereas the striations in *Figure 7a* suggest a 200–300 Å spacing. These striations, however, may be related to the 'superlattice' structure shown in *Figure 13d*.

The diffraction patterns in *Figures 12b–d* and *13a* show an apparent doubling of the lattice in the *b* axis direction, with the extra reflections being of variable intensity. It is not clear, however, whether the $k = n + \frac{1}{2}$ reflections are from the 0 or first layer of the reciprocal axis. It is possible that the crystal is thin enough that reciprocal lattice rods from the *hk*1 reciprocal lattice plane are intersecting the sphere of reflection. If so, however, even though the 'extra' reflections would then be forbidden in an *hk*0 pattern, the lattice would still be doubled. Since the sheared patterns show many fewer *hk*0 reflections and no quadrant diffraction, they cannot be used to resolve the above question.

ACKNOWLEDGEMENTS

The research was supported, in part, by the donors to the Petroleum Research Fund administered by the American Chemical Society (F. R.) and the National Science Foundation through grant DMR-8920538 (B.-L. Y.).

REFERENCES

1 Rybnikar, F., Liu, J. and Geil, P. H. *Makromol. Chem. Phys.* 1994, **195**, 81
2 Liu, J., Rybnikar, F. and Geil, P. H. *J. Polym. Sci., Polym. Phys. Edn* 1992, **30**, 1469
3 Liu, J., Rybnikar, F. and Geil, P. H. in preparation
4 Rybnikar, F., Liu, J. and Geil, P. H. Paper presented at American Chemical Society Meeting, San Francisco, April 1992
5 Rybnikar, F., Liu, J. and Geil, P. H. Paper presented at 34th IUPAC Symposium on Macromolecules, Prague, July 1992
6 Rybnikar, F., Liu, J. and Geil, P. H. Paper presented at NATO Research Workshop on Crystallization of Polymers, Mons, Belgium, September 1992
7 Rybnikar, F., Liu, J., Geil, P. H. and East, A. J. Paper presented at American Physical Society Meeting, Seattle, WA, March 1993
8 Li, L. S., Lieser, G., Rosenau-Eishin, R. and Fischer, E. W. *Makromol. Chem., Rapid Commun.* 1987, **8**, 159
9 Li, L. S. *Makromol. Chem., Rapid Commun.* 1989, **10**, 307
10 Li, L. S. and Geil, P. H. *Proc. Elec. Micro. Soc. Am.* 1989, 340
11 Rybnikar, F., Yuan, B. L. and Geil, P. H. *Polymer* 1994, **35**, 1863
12 Dorset, D. L. *J. Macromol. Sci., Phys.* 1986, **25**, 1
13 Windle, A. H., Viney, C., Golombok, R., Donald, A. M. and Mitchell, G. R. *Faraday Discuss. Chem. Soc.* 1985, **79**, 55
14 Hanna, S. and Windle, A. H. *Polymer* 1988, **29**, 207
15 Golombok, R., Hanna, S. and Windle, A. H. *Mol. Cryst. Liq. Cryst.* 1988, **155**, 281
16 Biswas, A. and Blackwell, J. *Macromolecules* 1988, **21**, 52, 58, 3146
17 Liu, J., Rybnikar, F., East, A. J. and Geil, P. H. *J. Polym. Sci., Polym. Phys. Edn* 1993, **31**, 1923
18 Kachidza, J., Serpe, G. and Economy, J. *Makromol. Chem., Makromol. Symp.* 1992, **53**, 65
19 Rybnikar, F. unpublished data
20 Liu, J., Rybnikar, F. and Geil, P. H. *J. Macromol. Sci., Phys.* 1993, **B32**, 395
21 Lauritzen, J. L. and Hoffman, J. D. *J. Res. Natl Bur. Std A* 1960, **64**, 73; and subsequent papers